

## **DYNAMIC PROPERTIES OF 40HM STEELS AT HIGH STRAIN RATES**

### **Summary**

When designing ballistic shields, it is of significance to know how materials behave at high strain rates. The paper presents results of the experimental investigation into the influence of the strain rate on the dynamic yield point of 40HM chromium-molybdenum steel. The behaviour of a material differs depending on impact speed, even if the impact energy remains the same. Dynamic tests were conducted on two specimens using two testing stations: a station equipped with a rotary hammer for testing at a speed reaching 40 m/s and a station accelerating the specimen to a high speed (160 to 270 m/s) and launching it to impact a hard, non-deformable shield. The dynamic yield point was determined by using the Taylor theory. To determine the impact speed, an optical measurement method and a digital high-speed camera were used. The impact speed was determined on the basis of the analysis of recorded images using a specialized software program. The impact speed was adjusted experimentally depending on the behaviour of the specimen material. The basic criterion for selecting the impact speed was that the requirement was fulfilled that the cylinder – as a result of the impact – succumbs to an evident plastic deformation without a visible material integrity infringement. The questions of plastic deformation, temperature influence, strain rate and stress–strain relation require an analysis of the formation and effects of dislocations. The unified constitutive law called Johnson-Cook's law describes the relations between the material's tension and strengthening ratio, and between strain rate and temperature. The tests indicated that a strain rate increase considerably improves strength properties of 40HM steel.

*Key words:*        *steel, dynamic stretching and compression test, Taylor's theory, rotary hammer, Johnson-Cook's equation*

### **1. Introduction**

Modern protective structures are currently sensitive elements of floating vessels. Their task is to reduce the effect of a terrorist activity of using explosives or missiles aimed at specific areas of a vessel. The knowledge of the behaviour patterns of materials undergoing high speed impacts has a highly significant meaning for the design of ballistic shields.

Ballistic shields can be an integral part of a ship's hull or they can be a ship's equipment element that can be separated from the hull plating. However, in order to successfully perform

their tasks, the shields have to be produced of materials fulfilling both the function of a ballistic shield and of a ship's structural cover.

Strength calculations of such structures are performed with the aid of numerical methods and computer techniques that apply constitutive formulae describing the behaviour of a given material. These formulae contain specific parameters and material constants of a projectile and a shield which have to be determined experimentally or "selected", which, in turn, poses a serious problem for high strain rate. In order to specify the dynamic properties of materials intended for manufacturing ballistic shields, it is necessary to set up appropriate testing stations equipped with an apparatus enabling the determination of material properties at high strain rate. The test results will allow the numerical calculation to be verified and, in effect, the penetration of the examined materials to be estimated.

The performed experimental tests indicated that an increase in the load speed and, accordingly, strain rate causes a rise in the yield point value. The problem becomes more complex when it is necessary to determine the influence of the load speed on the strength in brittle conditions. One can predict an increase in strength due to an additional inertia resistance. An increase in the load speed results in the material becoming brittle.

Elastic deformation refers to extending the crystal structure without infringing its balance. Plastic deformation, on the other hand, is caused by the movement of atomic planes. Considering the above, it is necessary to determine the values of strains which are a prerequisite to move the planes with respect to each other. Dislocations play a significant role in plastic deformation. It has been established that the stresses needed to shift dislocations are significantly lower than the stresses necessary for complete shifting of a plane with respect to its vicinity. Due to the fact that dislocations trigger real deformations, the values of stresses are 10 to 100 times lower than theoretical shear stresses.

Generally, it is possible to identify three ranges of impact speed: low, medium and high. Material behaves differently depending on the impact speed. Its behaviour during an impact speed  $> 1$  m/s differs from the behaviour during an impact speed of 10 km/s, even if the impact energy remains the same [1].

Low speed impacts are characterized by speeds in the order of a few meters per second. The impact duration time is significantly longer than the time needed by an elastic wave in the material to reach the edge of the object. The low speed impact is called a quasi-static impact due to a similar distribution of stresses [1-5]. In this case, supporting conditions are decisive [2, 5]. Materials to be subjected to the impact testing at low speeds are tested with the Charpy pendulum impact test.

Medium speed impacts (sub-ballistic impacts) are characterized by speeds in the order of tens of meters per second. The impact duration time is shorter and it is even too short for an elastic wave in the material to reach the edge of the object [1-4]. A decisive factor in the reaction of the material is the propagation of elastic waves along the surface of the object [1-5]. In this paper the interval of the mean speed was 5 to 40  $\text{ms}^{-1}$ . The dynamic stretching test was carried out with a rotary hammer. The obtained results allowed the yield point ( $R_{ed}$  – dynamic yield point) and plasticity ( $A_{Ad}$  – dynamic strain) to be determined depending on the strain rate. Results of examples from a dynamic study of the impact of a rotary hammer on a selected hull steel, i.e. austenitic steel and aluminium alloys used in marine and off-shore structures, were presented in papers [6-11].

High speed impacts (ballistic impacts) are characterized by speeds in the order of few hundred meters per second. The impact duration time is comparable with the duration of the propagation of waves in the normal direction towards the surface of a material. Damage generally concentrates at the impact area, since elastic waves in the material do not have time to propagate and the main reason for the damage is the local exceeding of the yield point at the front of the wave [1-4, 12]. Examples of this class of impacts include gunfire from firearms, projectile fragments or mid-air collisions of fast flying aircraft [13].

To determine dynamic properties of materials used for marine and off-shore structures, it is necessary to recognize the behaviour of the material exposed to impact loads, which is especially significant for navy vessels. In light of the above, structural materials should be loaded with speeds exceeding  $100 \text{ ms}^{-1}$  in order to discuss dynamic properties of a material at high strain rate.

Steel is a material that is used, among other purposes, to build energy-absorbing components as well as structural elements of armour for military uses. Therefore, a study on the properties of steel was carried out within a wide range of strain rate.

The paper presents two original methods for determining dynamic properties of 40HM steels. A rotary hammer was used for the stretching speed of  $40 \text{ ms}^{-1}$ , while the pyrotechnic method was used for the compression speed above  $200 \text{ ms}^{-1}$ . The research allowed the mechanical properties of 40HM steels for deformation speeds from 0 to  $300 \text{ ms}^{-1}$  to be determined.

Hypervelocity impacts are characterized by speed exceeding 1 km/s. At these speeds, the density of energy on a small area is so high that the strength of the material is exceeded by many orders of magnitude, the material begins to flow thermal effects connected with the energy transformation become significant and material evaporation is even possible. Such events usually affect space objects (satellites, space shuttles, etc.) [2, 3, 14].

Available literature contains scarce information on the relationship between strain rate and material strengthening mechanisms [15, 16]. The phenomenon of strengthening under the influence of high strain rate is explained on the basis of plastic deformation dislocation mechanisms [17-20, 21]. Such behaviour is caused by convergence of various dislocation mechanisms activated thermally [22]. The effects of the action of high strain rate include a decrease in the amount of cross-slip type dislocations, an increase in the frequency of occurrence of screw dislocations, an increase in the number of spot defects and a decrease in the efficiency of dynamic recovery [23]. The author observed the similarity between the structures forming under the influence of a high strain rate and the structures forming under a quasi-static load at low temperatures or metals with the low stacking fault energy. Such a similarity results from the uniformity of dislocation distribution, a decrease in the grain size and an increase in disorientation of dislocation cells with a higher number of dislocations remaining within the cells [21, 23].

In this paper, the problem has been illustrated with the example of chromium-molybdenum steel intended for use in the shipbuilding industry. The objective of the investigation was to determine stress-strain characteristics of the examined 40HM steel at various strain rates.

This objective has been accomplished by conducting dynamic stretching test and estimating the dynamic properties of shipbuilding materials, i.e. 40HM steel, at various strain rate. The paper presents theoretical bases of the problem and examinations of the influence of load speed on the physical properties of the material or the so called effect of material susceptibility on the strain rate.

## 2. Bases of the dislocation of the material deformation and dynamic yield limit

The phenomena of plastic deformation, influence of the temperature, strain rate, and stress-strain relation require an analysis of the dislocation formation and effects. Dislocation density  $\rho_D$  is defined as the length of the dislocation line (m) per a unit volume ( $\text{m}^3$ ).

The estimation of the deformation connected with the dislocation motion is performed on a specimen with a rectangular cross section of  $2,0 \times 10$  mm and 50 mm in length, subjected to a static tensile test. The volume of the specimen is  $V = 1000 \text{ mm}^3 = 10^{-6} \text{ m}^3$ . For a copper specimen, the Burgers vector is  $b = 0,256 \cdot 10^{-9} \text{ m}$ , for ferrite it is  $b = 0,248 \cdot 10^{-9} \text{ m}$  and for molybdenum it is  $b = 0,2725 \cdot 10^{-9} \text{ m}$ . The deformation caused by the dislocation motion is [24]:

$$\varepsilon = \rho_D b l, \quad (1)$$

where:

$l$  – distance covered by the dislocation.

The differentiation of the expression (1) by time yields a form of the Orowan formula [24, 25]  $d\varepsilon/dt = \dot{\varepsilon} = \rho_D b v$ , where  $v$  – denotes the mean dislocation velocity.

If the molybdenum specimen features a single dislocation whose size is 2 mm (specimen thickness) and which moves by 10 mm (total width of the specimen), the value of the deformation is:

$$\varepsilon = \rho_D b l = \frac{0,002 \text{ m}}{10^{-6} \text{ m}^3} (0,2725 \cdot 10^{-9} \text{ m})(0,010 \text{ m}) = 5,45 \cdot 10^{-9}.$$

It follows that a single dislocation causes a very small deformation. Taking into consideration a specimen in which the number of dislocation motions ranges from millions to billions of dislocations, a real deformation occurring in a mechanical test [24] is obtained. The simplest model expressing the relationship between stress and deformation can be written as an energy law [24]:

$$\sigma = K \varepsilon^n, \quad (2)$$

where:

$\varepsilon$  – strain,

$K, n$  – constant values, for example  $n \cong 0,5$  - for copper alloys and  $n \cong 0,15$  for some types of steel [24].

Due to its imperfection, formula (2) was subjected to numerous modifications [24]. Finally, the unified constitutive law known as Johnson-Cook's law was obtained and it has the following formula [24, 26]:

$$\sigma = (A + B \cdot \varepsilon^n) \left[ 1 - \left( \frac{T - T_r}{T_m - T} \right)^m \right] (1 + C \ln \dot{\varepsilon}) \quad (3)$$

where:

$T_r$  – reference temperature (ambient temperature),  $T_m$  – melting point,  
 $A, B, C, m, n$  – constant values.

In formula (3), the stress depends on the material strengthening ratio, strain rate and temperature. Constant values in formula (3) for a given type of material can be taken from literature [24, 27].

The dynamic yield point of the examined steel was determined on the basis of a theory developed in [28]. According to this theory, the results of geometrical measurements of a cylindrical specimen after its impact on a hard, non-deformable shield (plate) with the knowledge of the material density and velocity of its impact against the shield (Fig. 1) allow the dynamic yield point to be determined [29]. The examined specimens of the 40HM steel were accelerated to the linear velocity ranging from 160 to 270 m/s. Fig. 1 presents a schematic drawing showing the method for estimating the dynamic yield limit  $R_{ed}$ .

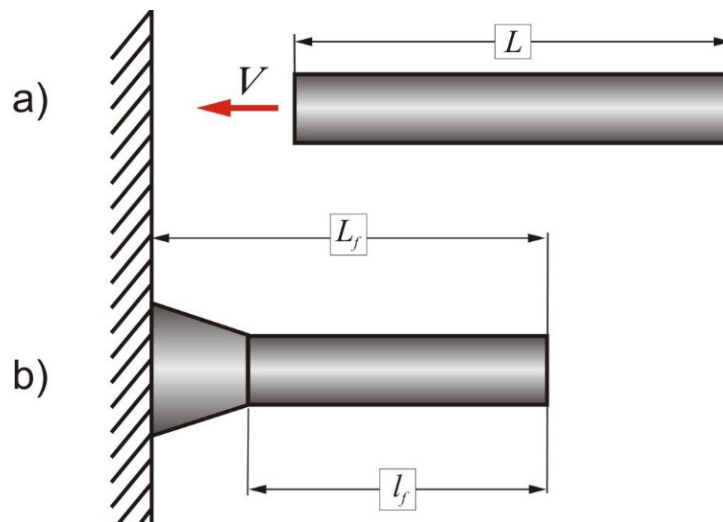


**Fig. 1** Schematic drawing of the Taylor method: a) geometry of the specimen prior to impact, b) geometry of the specimen after impact,  $\rho$  – density of the cylindrical specimen material;  $V$  – impact speed;  $L$  – length of the specimen prior to impact;  $L_f$  – total length of the specimen after impact;  $l_f$  – length of the non-deformed section of the specimen [30].

The primary form of the Taylor formula was subjected to numerous modifications [31, 32]. Finally, the formula describing the dynamic yield point of a material can be written as:

$$R_{ed} = \frac{\beta^s \rho V^2}{1 - \frac{l_f}{L}} \tag{4}$$

where:

$\beta^s$  – root of the equation  $a\beta^2 + b\beta + c = \beta d \ln\left[\frac{1 + \beta}{(l_f/L)\beta}\right]$  where  $a, b, c, d$  factors were calculated on the basis of the following relation:

$$a = \left(1 - \frac{l_f}{L}\right)^2 \left(\frac{L_f}{L} - 1\right) = -\left(1 - \frac{L_f}{L}\right) \left(1 - \frac{l_f}{L}\right)^2, \quad d = \left(\frac{l_f}{L}\right) \left(1 - \frac{l_f}{L}\right),$$

$$b = \left(1 - \frac{l_f}{L}\right) \left[2\left(\frac{L_f}{L}\right) - \left(\frac{l_f}{L} - 1\right)\right], \quad c = \left(\frac{L_f}{L}\right) - \left(\frac{l_f}{L}\right). \tag{5}$$

Relation (4) with the determined values of the factors (5) allows the dynamic yield point of the examined steel to be determined.

### 3. The investigation

Static and dynamic testings aiming at determining the yield point were conducted on the high-alloy chromium-molybdenum steel 40HM, marked as 0H18N9S according to PN standard, 42CrMo4 according to EN/ISO standard, or 4140 according to AISI standard. Mechanical properties of the 40HM steel are:

- $R_m = 1040$  MPa,  $R_e = 880$  MPa,  $A_4 = 10\%$ ,  $Z = 42\%$ ,  $E = 2.04 \cdot 10^5$  MPa [33].

Table 1 contains the chemical composition of the examined steel.

**Table 1** Chemical composition of high-alloy chromium-molybdenum steel 40HM [33].

C	Mn	Si	P	S	Cr	Ni	Mo	W	V	Cu
0.38- 0.45	0.4- 0.7	0.17- 0.37	max 0.035	max 0.035	0.9- 1.2	max 0.3	0.15- 0.25	max 0.2	max 0.05	max 0.25

Dynamic tests on the steel were conducted for two ranges of impact speeds:

- a) Medium speed of up to 40 m/s – specimens were subjected to stretching test using a rotatory hammer;
- b) High speed of up to 260 m/s – specimens were subjected to compression testing using the Taylor method.

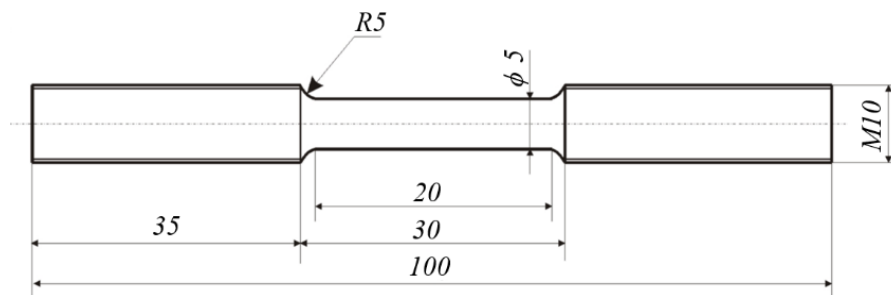


**Fig. 2** Geometry of the specimens subjected to static and dynamic stretching test with a rotary hammer.

The shape and dimensions of the specimens subjected to stretching test at medium speeds reaching up to 40 m/s can be seen in Fig. 2.

The static stretching test was carried out on an electrohydrodynamic testing machine MTS 810.12, controlled by a Test Star II computer device, while the dynamic stretching test was carried out using a rotary hammer.

The examinations of the dynamic properties of the tested steel were performed using a rotary hammer as a tool at the stretching speed reaching  $40 \text{ ms}^{-1}$ . Force  $F(t)$  was registered on the dynamometer applying the principle of the Hopkinson-Kolski bar that had a mounted set of strain gauges. The operational registration of the deformations  $\Delta l(t)$  of the specimen was carried out with an optoelectronic system measuring the displacement  $W(t)$  of the spreader beam and thus the deformation of the oscilloscope Le Croy Ls-140. Specimens with a diameter of 5 mm and the measurement base of 20 mm with M10 threaded grips were used in the tests. Strength properties were determined from the dynamic stretching tests on the basis of the maximum force transferred by a specimen ( $R_{md}$ ) and the force of the first loss of stability ( $R_{ed}$ ). A detailed description of the measurement station and the methods for result registration can be found in paper [33].

The pyrotechnical propulsion method using an 8 mm smoothbore barrel rifle was used to impact the cylindrical specimens. The distance between the muzzle of the rifle and the

surface of the target was approximately 350 mm. For high compressive speed reaching up to 270 m/s, the cylindrical specimens whose shapes and dimensions can be seen in Fig. 3a were prepared. A cylindrical specimen was placed in a shell (Fig. 3b), which was previously filled with a weighted portion of gunpowder whose mass was calculated with the aid of the numerical code applied to solve the problem of internal ballistics. The use of various weighted portions of gunpowder resulted in varied propulsion conditions (impact speed).

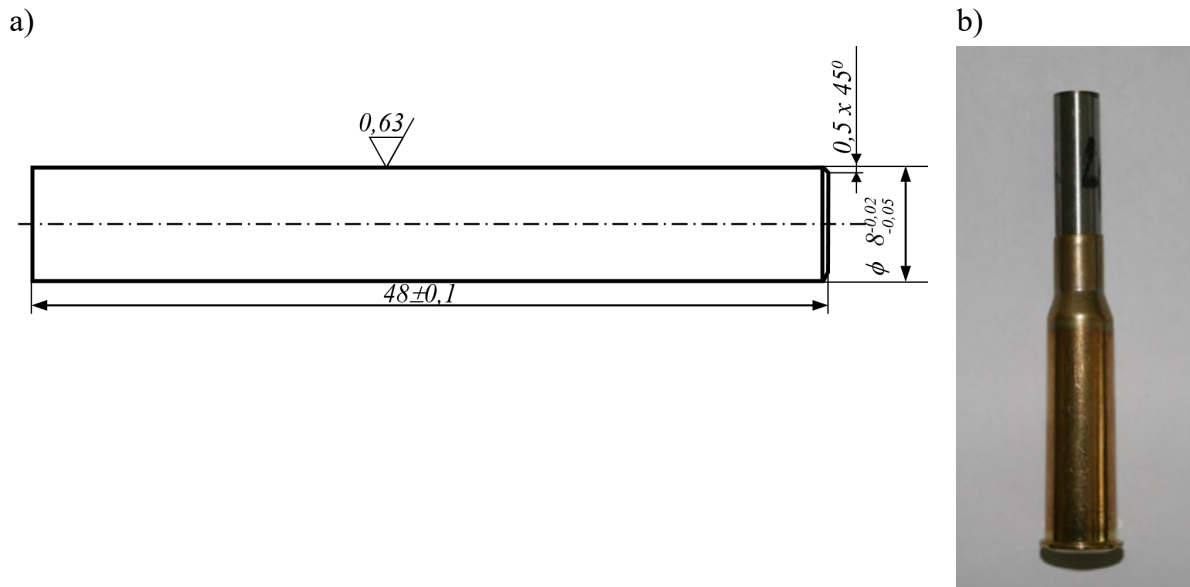


**Fig. 3** Dimension of the testing specimen and an image of the specimen placed in a shell [30].

The dynamic testing on the cylindrical specimens of the 40HM steel was performed on the station presented in Fig. 4.

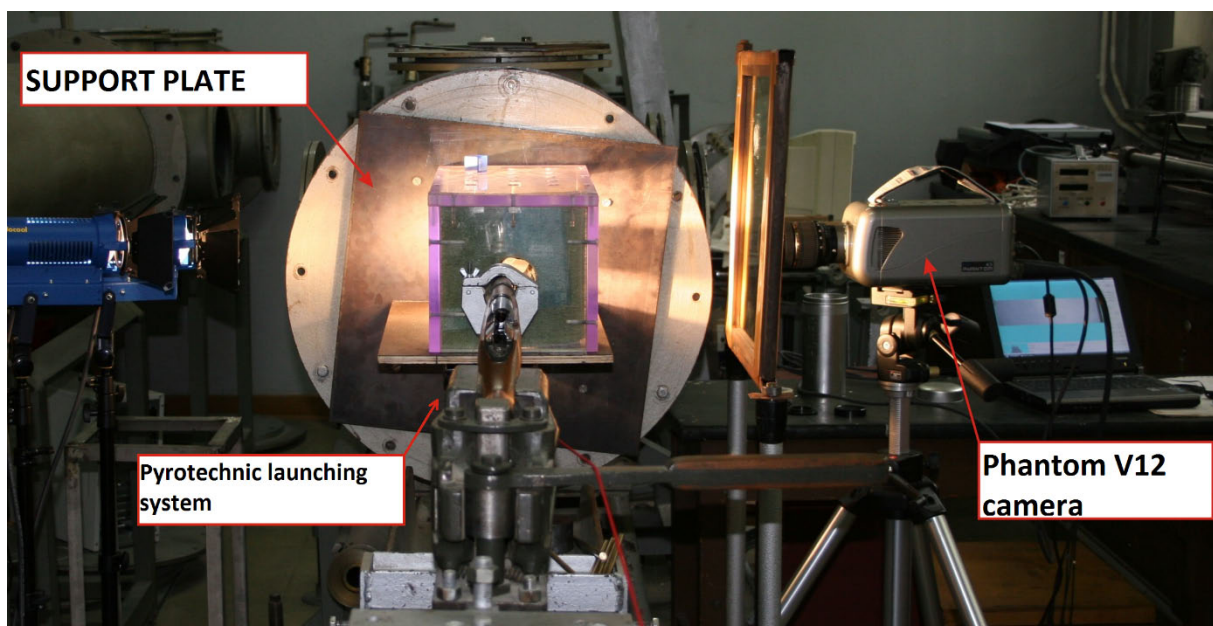


**Fig. 4** Station for dynamic deformation of cylindrical specimens [30].

In order to determine the impact speed, the optical measurement method based on the recording of the motion of the cylinder against a certain measurement section was used

directly before the cylinder impact on the non-deformable shield. A high-speed digital camera Phantom v12 was used in the test. The impact speed was determined through the analysis of the recorded images (film clips) using a specialized computer software program, on the basis of the average of the results obtained from the analysis of three images obtained from the software. The impact speed was adjusted experimentally depending on the behaviour of the specimen material. The basic criterion for selecting the impact speed was the requirement that the cylinder – as a result of the impact – succumbs to an evident plastic deformation without a visible crack in the material. Additionally, the terminal speeds of impact at which evident cracks in the deformed section of the cylinder appeared were estimated for the tested steel.

The tests were performed by shooting the cylinders at targets made of the maraging N18K9M5t steel. The target dimensions were as follows: diameter – 85 mm, thickness – 30 mm. The target material was 55 HRC. In order to maintain the testing conditions approximating the assumptions of the Taylor theory, the surface of the target was machined by means of grinding so that its surface roughness was appropriately low. Additionally, prior to each test, the targets were covered with a grease-based lithium soap, graphite and molybdenum disulphide. In turn, after each test the surface of the target was cleaned and examined. If any deformation or damage to the target surface was found, a subsequent test was performed in another section of the target area at a certain distance from the areas subjected to impact [30].

The basis for determining the dynamic yield point of the examined materials was the measurement of the total length of the cylinder after the impact  $L_f$  and the length of the non-deformed section of the cylinder  $l_f$ .

#### 4. Results of the experiments and analysis of the results

On the basis of the conducted experiments static and dynamic yield point of the 40HM steel was determined for stretching/compression speed ranging from 10 to 270 m/s.

Examples of graphs showing the results of the stretching test for the stretching speed of  $40 \text{ ms}^{-1}$  performed with a rotary hammer and recorded on a digital oscilloscope can be seen in Fig. 5.

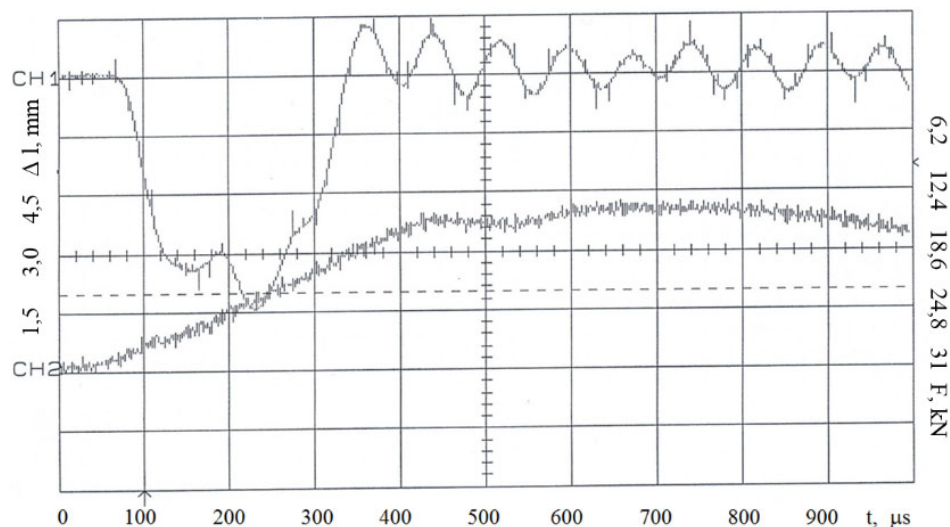


**Fig. 5** Relation between force and time  $F(t)$ –CH1 and displacement  $\Delta l(t)$ –CH2 for 40 HM steel specimen ( $\phi 5 \times 20 \text{ mm}$ ) dynamic stretching test with a rotary hammer, stretching speed  $V=40 \text{ ms}^{-1}$  [33].

The results included in the end report [33] were processed on the basis of the graphs recorded on a digital oscilloscope. The results of the measurements of the 40HM steel specimens tested with a rotary hammer with the speed range  $v=0\div 40\text{ ms}^{-1}$  are presented in Table 2.

**Table 2** Value of the yield point and strain in static and dynamic stretching test  $R_e, R_{ed}$  of 40HM steel according to results from [33].

Specimen diameter	$5.0^{+0.1}$				
Stretching speed, m/s	$\approx 0$	10	20	30	40
$R_e, R_{ed}$ , MPa	880	1000	1060	1100	1160
$A_4, A_{4d}$ , %	10	11	12	14	16

The course of the impact and the deformation process of the specimens at speeds ranging from 160 to 270 m/s were recorded with a high-speed digital camera. Fig. 6 presents examples of selected frames showing the course of the impact of specimen no. 1 (Table 3).

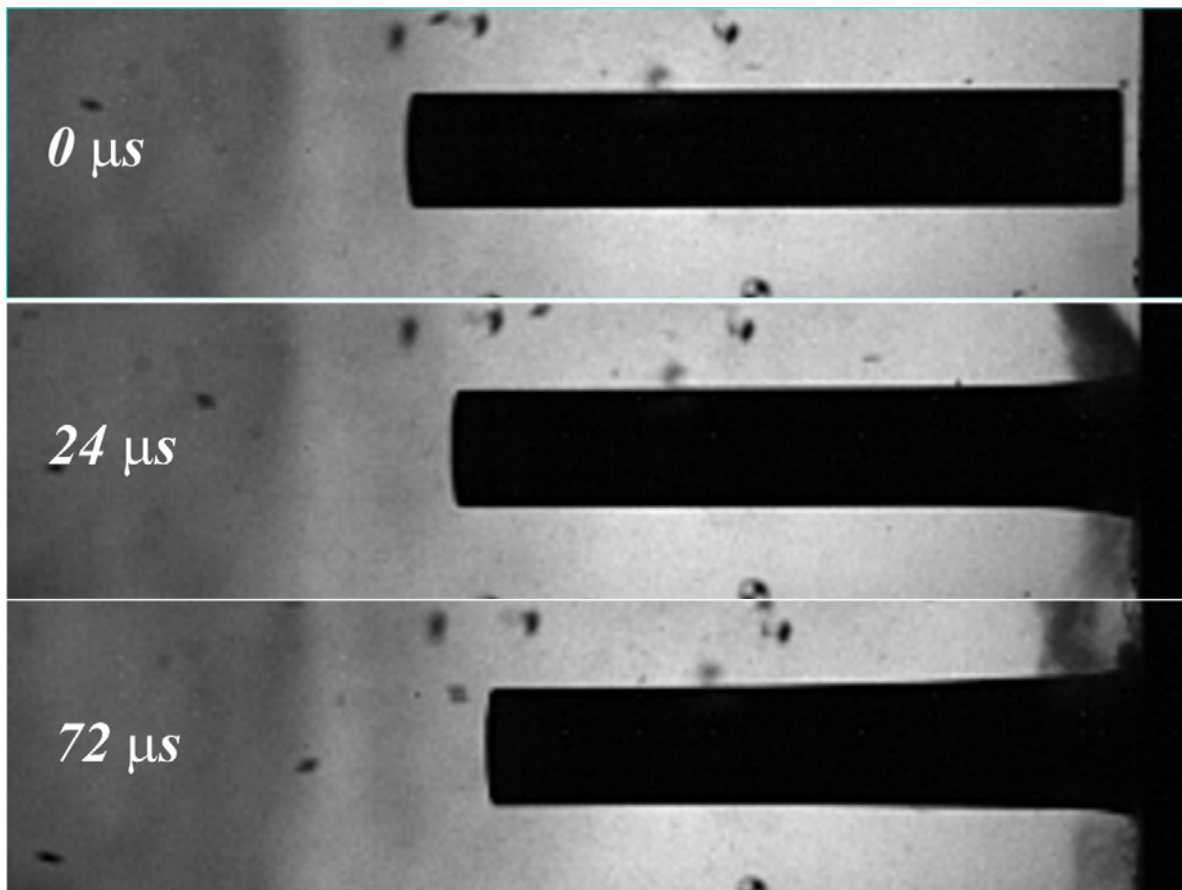


**Fig. 6** Selected film frames showing the course of plastic deformations of specimen no. 1 made of 40HM steel.

The strain rate of the specimens was determined on the basis of relation [28]:

$$\dot{\varepsilon} = V/2(L - l_f) \quad (6)$$

Table 3 contains the results of the tests of dynamic yield point for the specimen compression speed ranging from 160 to 270 m/s.

**Table 3** List of measurements and calculation results for 40HM steel specimens for compression speeds of 160 ÷ 270 m/s.

Specimen number	Diameter, mm	Initial length $L$ , mm	Speed $V$ , m/s	Final length $L_f$ , mm	Distance $l_f$ , mm	Dynamic yield point $R_{ed}$ , MPa
1	7.936	48.032	160.35	43.727	17.75	1244
2	7.962	48.023	178.62	42.855	16.8	1261
3	7.966	47.808	202.16	41.681	15.65	1332
4	7.894	48.004	265.43	38.270	12.2	1363
5	7.946	47.977	275.70	37.567	11.24	1375

The performed analysis of the dynamic deformation (strain rate from  $2.65 \cdot 10^3 \text{ s}^{-1}$  to  $3.75 \cdot 10^3 \text{ s}^{-1}$ ) of specimens of the examined steel indicated that this type of steel exhibits very good plastic properties. This is proved by a large swelling in the front section of the cylinder and the fact that the specimens were not fragmented as a result of the impact. The examined steel showed small cracks or hardly discernible strips of adiabatic shearing only when the propelling speed exceeded the value of approximately 260 m/s.

The front surfaces of the test cylinders launched at high speed did not exhibit any discolouration. The lack of temperature-induced discoloration can be justified by the fact that in the case of the 40HM steel the plastic deformation zone encompasses a major part of the cylinder.

On the basis of the obtained results of the experiments presented in graphs and tables it was found that the stretching speed of the tested specimens of the 40HM steel considerably influences the improvement in its strength properties. The characteristics of the dynamic stretching test of the 40HM steel specimens are placed much higher than the curves obtained during the static stretching test.

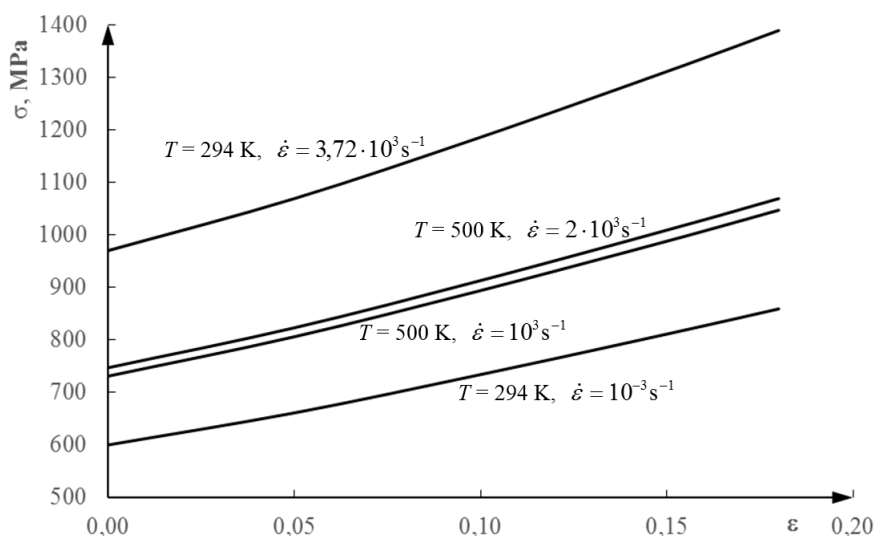
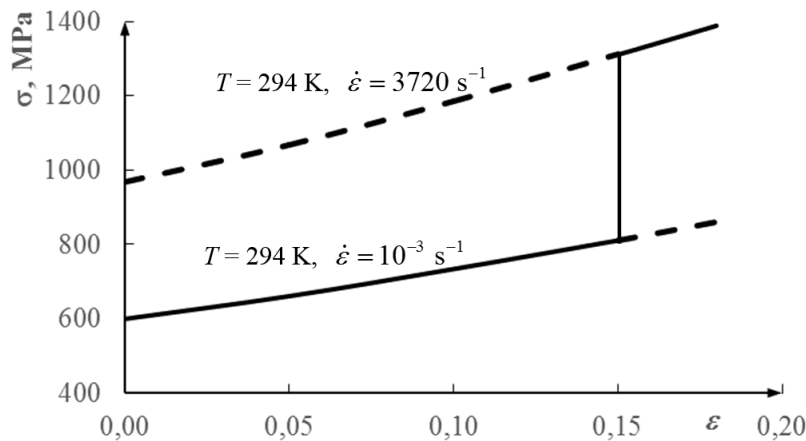
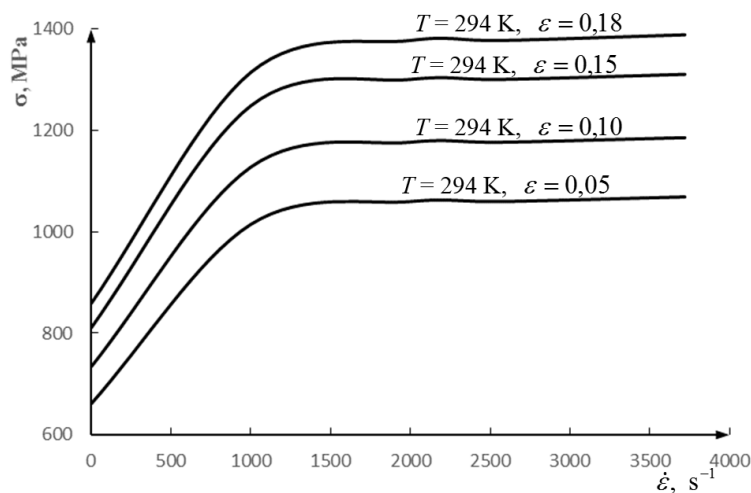
**Fig. 7** Stress–strain curves for 40HM steel, applying Johnson–Cook deformation model (relation 3).

Fig. 7 presents stress–strain curves of several strain rate and two constant values of temperature, described with the aid of the Johnson-Cook law for 40HM steel (3). Strength tests of the 40HM steel at an elevated temperature ( $T = 500 \text{ K}$ ) were not conducted. By applying formula (3) it is possible to predict the character of the curve. The results obtained from the experiments and the application of the Johnson-Cook formula confirm that the material yield point increases with an increase in the stretching/compression strain rate, which is associated with the dislocation processes described in Section 1.



**Fig. 8** Stress–strain curves for two-stage loading at two various strain rate and constant strain value equal  $\epsilon = 0,15$  determined on the basis of Johnson-Cook law for 40HM steel (relation 3).

The Johnson-Cook law for 40HM steel (3) allows predicting the behaviour of the material at various strain and load speed. For example, the specimen was initially loaded at an ambient temperature with the strain rate  $\dot{\epsilon} = 0,001 \text{ s}^{-1}$  to the strain value equal  $\epsilon = 0,15$ . Next, the strain rate was increased to the value of  $\dot{\epsilon} = 3720 \text{ s}^{-1}$ . Fig. 8 presents the predicted stress–strain curve (solid line) for two-stage loading on the basis of formula (3). The Johnson-Cook model enables the strain–stress transition from the value on the lower curve of the strain rate directly to the higher value of the strain rate curve to be described [24].



**Fig. 9** Stress–strain rate curves for various values of strain of 40HM steel.

Fig. 9 presents stress–strain rate curves at a constant temperature and various values of strain. The curves evidently illustrate the increase in the strength of the tested steel with an

increase in the strain rate. These are the curves described on the basis of the Johnson-Cook model (3).

As far as mechanical properties of the examined chromium-molybdenum steel are concerned, the increase in the stretching/compression speed causes an evident increase in the yield point. The ratio of maximum values of the dynamic yield point  $R_{ed}$  (for  $v = 275 \text{ ms}^{-1}$ ) to the static yield point  $R_e$  for 40HM steel is  $R_{ed} / R_e = 1,56$ .

## 5. Conclusions

The static or dynamic stretching/compression testing is accompanied by the cracking/damaging of the material especially in the fracture area in the vicinity of the so called necking. The damage can be defined by a function depending on the stresses, plastic deformation, plastic work, pressure, strain rate and temperature. The dynamic modelling of cracking requires appropriate models of the nucleation process and void growth. The nucleation of microscopic damage refers to micro-cracks that appear with the material's non-homogeneities, such as second phase particles, grain and sub-grain boundaries and the previously occurring flow of the material, especially with respect to the separation of precipitates from the matrix.

The examined steels have very good dynamic plasticity. 40HM steel shows strong susceptibility to strengthening under the influence of the dynamic deformation.

On the basis of the obtained results of the experiments one can state that an increase in the strain rate causes an evident increase of the yield point at dynamic stretching/compression in relation to static stretching/compression ( $R_{ed} / R_e = 1,56$ ). On the assumption that the basis of the flow of the metal is a thermally activated process which defines the dislocation motion through the crystal lattice containing point defects, the tensile velocity is often described in a form of the Arrhenius formula.

The conclusions drawn from the static and dynamic testing constitute a basis for modelling the dynamic deformation of steel as an elastic/viscoplastic material.

## REFERENCES

- [1] Abrate S., Impact on composite structures, Cambridge University Press, Cambridge **1998**.
- [2] Naik N.K., Shirao. P., Composite structures under ballistic impact, *Composite Structures* **2004**, 66, 579-590. <https://doi.org/10.1016/j.compstruct.2004.05.006>
- [3] Cheeseman B.A., Bogetti T.A., Ballistic impact into fabric and compliant composite materials, *Composite Structures* **2003**, 61, 161-173. [https://doi.org/10.1016/s0263-8223\(03\)00029-1](https://doi.org/10.1016/s0263-8223(03)00029-1)
- [4] Olsson R., Mass criterion for wave controlled impact response of composite plates, *Composites: Part A* **2000**, 31, 879-887. [https://doi.org/10.1016/s1359-835x\(00\)00020-8](https://doi.org/10.1016/s1359-835x(00)00020-8)
- [5] Bland P.W., Dear J.P., Observations on the impact behaviour of carbon-fibre reinforced polymers for the qualitative validation of models, *Composites: Part A* **2001**, 32, 1217-1227. [https://doi.org/10.1016/s1359-835x\(01\)00076-8](https://doi.org/10.1016/s1359-835x(01)00076-8)
- [6] Charchalis A., Kyzioł L., Testing 10GHMBA steel for vessel ballistic shields, International Scientific Congress on Powertrain and Transport Means, *Journal of KONES*, Vol. 18 No. 2, **2011**, pp.69-76. <https://doi.org/10.5604/12314005.1138658>
- [7] Kyzioł L., Jurczak W., Modelling of The Ship Structural Ballistic Shields From 10GHMBA Steel, *Solid State Phenomena* Vol. 180, **2012** pp 303÷312. Trans Tech Publications, Switzerland. <https://doi.org/10.4028/www.scientific.net/ssp.180.303>
- [8] Kyzioł L., Garbacz G., Zależność wytrzymałość stali austenitycznej 0H18N9S od szybkości odkształcenia, *Logistyka*, 6 **2014**, str. 6520-6528.

- [9] Kyzioł L., The influence of temperature and strain rate on the strengthening of metallic materials, *Journal of Kones*, **2016**, Vol. 23, No 1, pp. 199-206. <https://doi.org/10.5604/12314005.1213566>
- [10] Kyzioł L.: Determination of the mechanical threshold stress in relation to austenitic stainless steel 00H21AN16G5M4Nb, *High Temperature Material Processes*, Vol.21, Issue 1, **2017**, pp.25-35. <https://doi.org/10.1615/hightempmatproc.2017019344>
- [11] Kyzioł L.: The influence of strain rate on the strength the constructional low-alloy steel, *МЕХАНИКА МАШИИ, МЕХАНИЗМОВ И МАТЕРИАЛОВ*, № 3 (40) **2017**, pp. 72-76.
- [12] Cantwell WJ, Morton J. The impact resistance of composite materials – a review, *Composites* **1991**, 22, 347-362. [https://doi.org/10.1016/0010-4361\(91\)90549-v](https://doi.org/10.1016/0010-4361(91)90549-v)
- [13] Davies GAO, Zhang X, Zhou G, Watson S. Numerical modelling of impact damage, *Composites* **1994**, 25, 342-350. [https://doi.org/10.1016/s0010-4361\(94\)80004-9](https://doi.org/10.1016/s0010-4361(94)80004-9)
- [14] Bernhard R.P., Christiansen E.L., Hyde J., Crews J.L., Hypervelocity impact damage into space shuttle surfaces, *International Journal of Impact Engineering* **1995**, 17, 57-68. [https://doi.org/10.1016/0734-743x\(95\)99835-f](https://doi.org/10.1016/0734-743x(95)99835-f)
- [15] Wyrzykowski W., Pleszakow E, Sieniawski J., Odkształcenie i pękanie metali, Wydawnictwo Naukowo-Techniczne, **1999**, Warszawa.
- [16] Przybyłowicz K., Strukturalne aspekty odkształcania metali, Wydawnictwo Naukowo-Techniczne, **2002**, Warszawa.
- [17] Gurrutxaga-Lerma B, Balint DS, Dini D, Sutton AP, The mechanisms governing the activation of dislocation sources in aluminum at different strain rates, *J. Mech. Phys. Solids*, **2015** 84:273–292. <https://doi.org/10.1016/j.jmps.2015.08.008>
- [18] Gurrutxaga-Lerma B, Balint DS, Dini D, et al, Attenuation of the dynamic yield point of shocked aluminum using elastodynamic simulations of dislocation dynamics, *Phys Rev Lett*, **2015**, 114:1–5. <https://doi.org/10.1103/physrevlett.114.174301>
- [19] Zerilli FJ, Armstrong RW, A constitutive equation for the dynamic deformation behavior of polymers, *J Mater Sci*, **2007**, 42:4562–4574. <https://doi.org/10.1007/s10853-006-0550-5>
- [20] Armstrong RW, Arnold W, Zerilli FJ, Dislocation mechanics of shock-induced plasticity, *Metall Mater Trans A Phys Metall Mater Sci*, **2007** 38 A:2605–2610. <https://doi.org/10.1007/s11661-007-9142-5>
- [21] Stopel M., Projektowanie konstrukcji mechanicznych poddanych działaniu obciążeń narastających z dużą prędkością, Uniwersytet Technologiczno-Przyrodniczy, **2018**, Bydgoszcz.
- [22] Fan Y, Osetskiy YN, Yip S, Yildiz B, Mapping strain rate dependence of dislocation-defect interactions by atomistic simulations, *Proc Natl Acad Sci USA*, **2013** 110:17756–61. <https://doi.org/10.1073/pnas.1310036110>
- [23] Gray GT, High-Strain-Rate Deformation: Mechanical Behavior and Deformation Substructures Induced, *Annu Rev Mater Res* , **2012** 42:285– 303. <https://doi.org/10.1146/annurev-matsci-070511-155034>
- [24] Follansbee P. S., Fundamentals of strength. Wiley, New Jersey, 2014.
- [25] Estrin E., Dislocation-density-related constitutive modeling, in unified constitutive laws of plastic deformation, Vol. 48, Krausz A. S. and Krausz K., eds. Academic Press , New York **2003**, pp. 171-273. <https://doi.org/10.1016/b978-012425970-6/50003-5>
- [26] Follansbee P. S., Huang J. C., and Gray G. T., Low-temperature and high-strain-rate deformation of nickel and nickel-carbon alloys and analysis of the constitutive behavior according to an internal state variable model, *Acta Metallurgica et Materialia*, Vol. 38, No.7, **1990**, pp. 1241-1254. [https://doi.org/10.1016/0956-7151\(90\)90195-m](https://doi.org/10.1016/0956-7151(90)90195-m)
- [27] Johnson G.R., Cook W.H., A constitutive model and data for metals subjected to large strains, high strain rates and high temperatures, Proceedings of the 7<sup>th</sup> International Symposium on Ballistics, The Hague, The Netherlands, April **1983**, pp. 541-548.
- [28] Taylor G., The use of flat-ended projectiles for determining dynamic yield stress I. Theoretical considerations. *Proc. Roy. Soc. London Series A.* **1948**, 194, 289. <https://doi.org/10.1098/rspa.1948.0081>
- [29] Whiffen A. C., The use of flat-ended projectiles for determining dynamic field stress II, Tests on various metallic materials, *Proc. Roy. Soc. London Series A.* **1948**, 194, 300. <https://doi.org/10.1098/rspa.1948.0082>
- [30] Janiszewski J., Wykonanie badań dynamicznych właściwości mechanicznych stali 10 GHMBA za pomocą metody Taylora, Sprawozdanie z pracy badawczej, WAT, Warszawa **2009**, pp. 16.
- [31] Jones S.E., P.P. Gillis P. P., Foster Jr. J. C., On the equation of motion of the unreformed section of a Taylor impact specimen, *J. Appl. Phys.* **1987**, 61, 499.

- [32] Janiszewski J., Koperski W., Materniak J., Starczewska A., Włodarczyk E., Oszacowanie dynamicznej granicy plastyczności wybranych stali łuskowych za pomocą uderzeniowego testu Taylora, *Biul. WAT* vol. LVI 1(645) **2007**.
- [33] Kyzioł L., Zatorski Z., Dobrociński S., Skrzydlak A., Bohn M., Wypych W., Michalski W. Dynamic characteristics of materials for marine structures, Final report from the work of pk. *CONSTRUCTOR*, stage I–III, AMW, Gdynia **2002–2004**.

Submitted: 27.02.2019

Accepted: 02.6.2019

Lesław Kyzioł  
kyziol@wm.umg.edu.pl  
Gdynia Maritime University, Faculty of  
Marine Engineering, Gdynia, Poland